

Crystal Structures of Polymerized Fullerenes AC_{60} , $A=K, Rb, Cs$ and Alkali-mediated Interactions

B. Verberck¹, K.H. Michel¹, and A.V. Nikolaev^{1,2}

¹*Department of Physics, University of Antwerp, UIA, 2610 Antwerpen, Belgium*

²*Institute of Physical Chemistry of RAS, Leninskii prospect 31, 117915, Moscow, Russia*

(October 22, 2018)

Starting from a model of rigid interacting C_{60} polymer chains on an orthorhombic lattice, we study the mutual orientation of the chains and the stability of the crystalline structures $Pmnn$ and $I2/m$. We take into account i) van der Waals interactions and electric quadrupole interactions between C_{60} monomers on different chains as well as ii) interactions of the monomers with the surrounding alkali atoms. The direct interactions i) always lead to an antiferrorotational structure $Pmnn$ with alternate orientation of the C_{60} chains in planes (001). The interactions ii) with the alkalis consist of two parts: translation-rotation (TR) coupling where the orientations of the chains interact with displacements of the alkalis, and quadrupolar electronic polarizability (ep) coupling, where the electric quadrupoles on the C_{60} monomers interact with induced quadrupoles due to excited electronic d states of the alkalis. Both interactions ii) lead to an effective orientation-orientation interaction between the C_{60} chains and always favor the ferrorotational structure $I2/m$ where C_{60} chains have a same orientation. The structures $Pmnn$ for KC_{60} and $I2/m$ for Rb- and CsC_{60} are the result of a competition between the direct interaction i) and the alkali-mediated interactions ii). In Rb- and CsC_{60} the latter are found to be dominant, the preponderant role being played by the quadrupolar electronic polarizability of the alkali ions.

I. INTRODUCTION

Alkali metal doped C_{60} (A_xC_{60}), $A=K, Rb, Cs$, forms stable crystalline phases (fullerenes) with a broad range of physical and chemical properties comprising superconductors and polymer phases. For a review, see Refs. [1–3]. In particular the $x = 1$ compounds [4] exhibit plastic crystalline phases with cubic rock-salt structure (space group $Fm\bar{3}m$) at high temperature ($T \geq 350$ K) and polymer phases [5–8] at lower T . In the latter case the C_{60} molecules are linked through a [2+2] cycloaddition [7], a mechanism originally proposed for photoinduced polymerization [9] in pristine C_{60} . From X-ray powder diffraction [7] it was concluded that the crystal structure of both KC_{60} and RbC_{60} was orthorhombic (space group $Pmnn$). Polymerization occurs along the orthorhombic \vec{a} axis (the former cubic [110] direction). The orientation of the polymer chain, taken as a rigid unit, is characterized by the angle ψ of the planes of cycloaddition with the orthorhombic \vec{c} axis. In the $Pmnn$ structure (Fig. 1a) the chains have alternating orientations $+\psi$ and $-\psi$, $|\psi| \approx 45^\circ$. Notwithstanding this apparent structural similarity the electronic and magnetic properties of KC_{60} on one hand and RbC_{60} and CsC_{60} on the other hand were found to be very different [2]. ESR and optical conductivity data [6,10] show that RbC_{60} and CsC_{60} exhibit a transition from a quasi-one-dimensional metal to an insulating magnetic state near 50 K, while KC_{60} stays metallic and nonmagnetic at low T . NMR spectra also did show marked differences between K- and Rb-, CsC_{60} polymers [11]. The contradiction between similar crystalline structures and different electromagnetic properties was resolved by single crystal X-ray diffraction and diffuse scattering studies [12].

While the space group $Pmnn$ is confirmed for KC_{60} , it is found that RbC_{60} is body-centered monoclinic with space group $I2/m$. In the latter structure, the polymer chains have the same orientation ψ (Fig. 1b) in successive (001) planes. High-resolution synchrotron powder diffraction [13] results have demonstrated that CsC_{60} has the same structure as RbC_{60} . Most recently a detailed structure of the polymer phase of K- and RbC_{60} has been performed by high-resolution neutron powder diffraction [14]. The distinct crystalline structures are confirmed and in addition a determination of the positions of the C nuclei demonstrates a distortion of the C_{60} monomers. The discovery of a metal-insulator phase transition by ESR spectroscopy in KC_{60} around $T = 50$ K and the concomitant appearance of a superstructure revealed by X-ray diffraction [15] demonstrate a subtle interplay of structure, dimensionality and electronic properties. In fact the nature of electrical conductivity in the AC_{60} compounds is still under debate. Previous electronic band structure calculations [16,17] suggest a three-dimensional dispersion of the electronic bands. However numerous experiments [3] are interpreted in terms of a quasi-one-dimensional conductor.

Concerning our understanding of the crystalline structure, a condensation scheme has been proposed for the phase transition from the orientationally disordered structure $Fm\bar{3}m$ to the orientationally ordered polymer phase $Pmnn$ on basis of a phenomenological Landau theory [18]. However, a microscopic description of this transition (which involves the cycloaddition process) is very complex. Already in the $Fm\bar{3}m$ phase, the charge transfer of one electron from the alkali atoms to the C_{60} molecules giving rise to a $A^+C_{60}^-$ crystal changes the electronic structure of the molecule. This change affects the

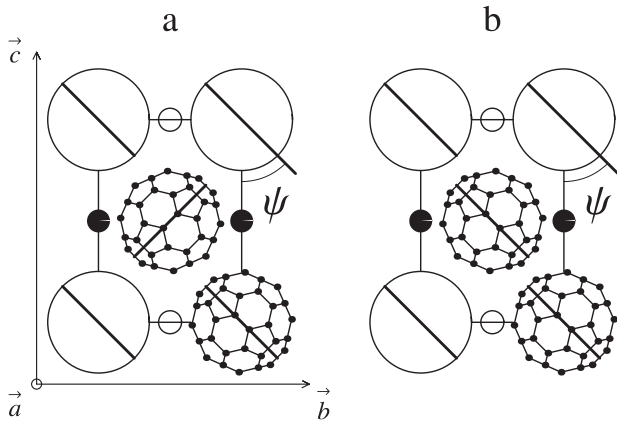


FIG. 1. Crystal structures projected onto the crystallographic (\vec{b}, \vec{c}) plane: (a) $Pmnn$, (b) $I2/m$. The thick bars represent the projection of the cycloaddition planes. Polymerization occurs along \vec{a} . The alkalis located in (\vec{b}, \vec{c}) planes and at $\pm a/2$ are denoted by full (+) and empty (-) circles.

orientation dependent interactions, in particular the crystal field, and favors polymerization [19]. The latter is a quantum-chemical process and within our view it is the driving mechanism for the phase transition. There remains the question why polymerized KC_{60} and $Rb-$, CsC_{60} have different crystal structures and different electronic properties and why pressure polymerized C_{60} has the same crystalline structure as KC_{60} . In the following we will essentially address the problem of the various crystalline structures. It turns out that the differences in structure can be related to the average radii of excited electronic d -states of the alkali cations. A preliminary account has been given as a letter [20]. There it was found that the direct electric quadrupole interactions between charged polymer chains in the alkali fullerides (the existence of electric quadrupoles on the chains is a consequence of the charge transfer between an alkali atom and a C_{60} monomer [21]) always favors the structure $Pmnn$ with alternating chain orientations. While this result agrees with experiment for the case of KC_{60} , it does not explain the monoclinic structure $I2/m$ of RbC_{60} and CsC_{60} . Hence it becomes necessary to take into account the role of the alkalis. In particular the specific quadrupolar polarizability of the alkali metal ions leads to an indirect interchain coupling which favors $I2/m$ with equal chain orientation. The competition between direct and indirect interactions then explains the structural differences between KC_{60} and RbC_{60} , CsC_{60} . In the present paper we will present several important extensions of the previous work.

Since polymerization leads to chains of D_{2h} symmetry, one has to investigate the role of van der Waals interactions (repulsive Born-Mayer and attractive London dispersion forces) for a configuration that is very different from the situation in orientationally disordered C_{60} . Potential energy calculations based on van der Waals forces between C_{60} polymer chains show that the energy

minimum is highly sensitive to the relative chain orientation [22]. We will show that the dominant term of the multipole expansion of the van der Waals interaction between different chains, corresponding to quadrupole-quadrupole interactions, always favors the orthorhombic $Pmnn$ structure too. Our study of the van der Waals interchain interactions is not only relevant for the structure of the AC_{60} compounds, where the direct interchain interactions are in competition with the alkali-mediated chain-chain interactions, but also for the understanding of the structure of polymerized C_{60} . There a “low pressure” orthorhombic phase was found to have the structure $Pmnn$ [23,24].

As a further extension we will study the coupling between rotational motion of the polymer chains and the lattice translations of the alkalis (TR coupling). Thereby we will obtain the shear mode that characterizes the monoclinic unit cell of RbC_{60} [14] and CsC_{60} [13]. However our calculations show that the indirect chain-chain interaction mediated by the displacements of the alkalis is relatively weak and is not able to account for the structural difference between KC_{60} and $Rb-$, CsC_{60} . The quadrupolar polarizability mediated interaction is the decisive mechanism.

The content of the paper is as follows. In Sect. II we formulate the rigid chain model of C_{60} polymer chains in the orthorhombic lattice (space group $Immm$). The sole degree of freedom of each chain is the rotation angle ψ about the long axis. Since the interchain potential is a function of the angles ψ , we perform a multipole expansion into symmetry adapted rotator functions (SARFs), taking into account the symmetry of the polymer chain (D_{2h}) and of the site. The direct interchain potential is studied for both Coulomb and van der Waals forces between monomers on different chains (Sects. II and III). These forces lead to Coulomb- and van der Waals type quadrupole-quadrupole interactions between chains. Studying the direct interaction potentials in Fourier space, we find that they always favor the structure $Pmnn$. Next (Sect. IV) we study the interactions of the C_{60} chains with the surrounding alkalis. We consider two types of interactions. Firstly the coupling of the rotations of the polymers with the alkali displacements (TR-coupling) via van der Waals and Coulomb forces, and secondly the coupling of rotations of the polymers with induced quadrupoles on the alkali cations (quadrupolar polarizability coupling). Both interactions lead to an effective rotation coupling between polymer chains, which always favors a ferrorotational structure $I2/m$. In the following, we study the competition between direct and indirect interactions and discuss the stability of structures (Sect. V). Finally (VI) conclusions are drawn. We discuss the unique properties of AC_{60} in comparison with ionic molecular crystals with small ions. The paper has three appendices, where we discuss: A) the orthorhombic lattice structure as a consequence of polymerization, B) details about the interchain potentials, C) the microscopic origin of the quadrupolar polarizability of the

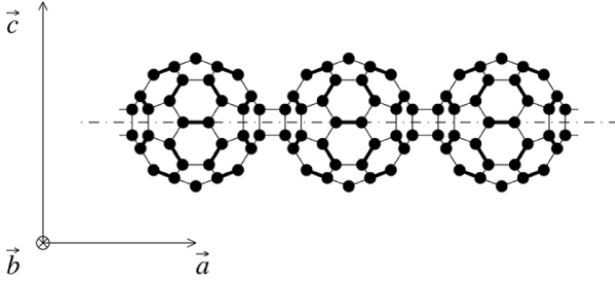


FIG. 2. Fragment of a C_{60} polymer chain, orientation $\psi = 0$.

cations.

II. RIGID CHAIN MODEL

We start from the assumption that the polymerization by stereospecific cycloaddition of C_{60} molecules in AC_{60} has occurred along the original cubic $[110]$ direction. Polymerization acts as a negative uniaxial stress along $[110]$. By using concepts of the theory of elasticity [25], we find that the cubic crystal is deformed into an orthorhombic one (point group D_{2h}). Taking the cubic $[110]$, $[1\bar{1}0]$, and $[001]$ as new ξ , η , ζ axes (orthorhombic \vec{a} , \vec{b} , \vec{c}) respectively, we find the deformations

$$\epsilon_{\xi\xi} = -\frac{K}{4dc_{44}} [c_{11}(c_{11} + c_{12} + 2c_{44}) - 2c_{12}^2], \quad (2.1a)$$

$$\epsilon_{\eta\eta} = \frac{K}{4dc_{44}} [c_{11}(c_{11} + c_{12} - 2c_{44}) - 2c_{12}^2], \quad (2.1b)$$

$$\epsilon_{\zeta\zeta} = Kc_{12}/d, \quad (2.1c)$$

where $d = c_{11}(c_{11} + c_{12}) - 2c_{12}^2$, $K > 0$. Details of the derivation are given in Appendix A. From the relations between the cubic elastic constants we see that $\epsilon_{\xi\xi} < 0$, $\epsilon_{\eta\eta} > 0$ and $\epsilon_{\zeta\zeta} > 0$, which corresponds to a contraction along the ξ direction (which we identify with the orthorhombic \vec{a} axis) and to elongations along the η and ζ directions (the orthorhombic \vec{b} and \vec{c} axes respectively). In the following we consider an orthorhombic lattice with space group $Immm$, with polymer chains oriented along the \vec{a} axis (Fig. 2). We take the chains as rigid units of D_{2h} symmetry where the sole degree of freedom is the rotation angle ψ about the chain axis \vec{a} . The assumption of a rigid chain is a reasonable first approximation, indeed vibrational density of states data on RbC_{60} obtained by inelastic neutron scattering exhibit a low energy external mode below 5 meV which is interpreted as arising from librations around the chain axis [26]. Inelastic neutron scattering results on the orthorhombic phase of KC_{60} are in close agreement with these results [27].

The mathematical formulation of our model of a polymerized crystal is as follows. We consider N C_{60} molecules located on a body-centered orthorhombic lattice, where the center of mass positions of the molecules

coincide with the lattice points. The lattice points are labeled by indices $\vec{n} = (n_1, n_2, n_3)$. These are either all integers or all half integer numbers, corresponding respectively to the corners and the center of the orthorhombic cell. The equilibrium position of the \vec{n} -th lattice point then reads

$$\vec{X}(\vec{n}) = n_1\vec{a} + n_2\vec{b} + n_3\vec{c}, \quad (2.2)$$

where \vec{a} , \vec{b} and \vec{c} are the orthorhombic lattice vectors. The molecules (monomers) in a polymer chain are oriented so that a twofold molecular axis coincides with the orthorhombic \vec{a} axis (ξ -direction). The number of chains is N_c , and the number of monomers within a chain is N_1 , hence $N = N_c N_1$. We define as standard orientation of a polymer chain the orientation where the plane of cycloaddition is parallel to the (\vec{a}, \vec{c}) planes of the orthorhombic crystal. The angle ψ then measures a counterclockwise rotation of the polymer about \vec{a} , the standard orientation corresponding to $\psi = 0$ (Fig. 2). Since it is sufficient to specify the indices $\vec{v} = (n_2, n_3)$ to address a polymer chain, and because all molecules along one chain have the same orientation, the rotation angle is independent of the index n_1 and is written as $\psi \equiv \psi(\vec{v})$. The interaction between chains is then formulated as a sum of two-body potentials $U(\vec{n}, \psi(\vec{v}); \vec{n}', \psi(\vec{v}'))$ between C_{60} monomers:

$$V = \frac{1}{2} \sum_{\vec{n}, \vec{n}'} U(\vec{n}, \psi(\vec{v}); \vec{n}', \psi(\vec{v}')). \quad (2.3)$$

This interaction depends on the mutual orientation of the chains. In order to describe the symmetry reduction (phase transition) from a hypothetical polymer crystal with structure $Immm$ (i. e. no preferential orientation angle $\psi(\vec{v})$) to $Pmnn$ or $I2/m$, we perform a multipole expansion of the potential in terms of SARFs $S_l(\vec{v}) \equiv S_l(\psi(\vec{v})) = \sin(l\psi(\vec{v}))$, $C_l(\vec{v}) \equiv C_l(\psi(\vec{v})) = \cos(l\psi(\vec{v}))$, l being the angular momentum quantum number. SARFs are the most appropriate variables for the description of orientation dependent properties in molecular solids [28–30]. Since in the present problem the assumption of a rigid chain leads to one single rotation angle ψ , our SARFs are particularly simple and correspond to planar rotator functions [31]. Symmetry of the chain for $\psi \rightarrow \psi + \pi$ implies that only even values of l occur. In lowest order of the multipolar index l we obtain

$$V = V_{QQ}^{RR} + V_{CF}, \quad (2.4)$$

with

$$V_{QQ}^{RR} = \frac{1}{2} \sum_{n_1, n_1'} \sum_{\vec{v}, \vec{v}'} J_{QQ}(n_1, \vec{v}; n_1', \vec{v}') S_2(\vec{v}) S_2(\vec{v}'), \quad (2.5a)$$

$$V_{CF} = \sum_{n_1, n_1'} \sum_{\vec{v}, \vec{v}'} v(n_1, \vec{v}; n_1', \vec{v}') C_2(\vec{v}). \quad (2.5b)$$

Here V_{QQ}^{RR} stands for the quadrupolar ($l = 2$) rotation-rotation interaction. The quadrupolar function S_2 , which

is uneven in $\psi(\vec{\nu})$, is an appropriate order parameter. The coefficients J_{QQ} are obtained from

$$J_{QQ}(n_1, \vec{\nu}; n'_1, \vec{\nu}') = \frac{1}{\pi^2} \int_0^{2\pi} d\psi(\vec{\nu}) \int_0^{2\pi} d\psi(\vec{\nu}') \times U(\vec{n}, \psi(\vec{\nu}); \vec{n}', \psi(\vec{\nu}')) S_2(\psi(\vec{\nu})) S_2(\psi(\vec{\nu}')). \quad (2.6)$$

The term V_{CF} accounts for the crystal field. It is the potential experienced by a central chain with orientation $\psi(\vec{\nu})$ where the surrounding chains are taken in cylindrical approximation ($l = 0$). The coefficients v are given by

$$v(n_1, \vec{\nu}; n'_1, \vec{\nu}') = \frac{1}{2\pi^2} \int_0^{2\pi} d\psi(\vec{\nu}) \int_0^{2\pi} d\psi(\vec{\nu}') \times U(\vec{n}, \psi(\vec{\nu}); \vec{n}', \psi(\vec{\nu}')) C_2(\psi(\vec{\nu})). \quad (2.7)$$

For a C_{60} monomer on a site $(n_1, \vec{\nu})$ we consider the interactions J_a with the two monomers at $(n_1 \pm \frac{1}{2})$ on the four neighboring chains $(n_2 \pm \frac{1}{2}, n_3 \pm \frac{1}{2})$ and the interactions J_b with the one monomer on each of the chains $(n_2 \pm 1, n_3)$.

We introduce Fourier transforms

$$S_2(\vec{n}) = \frac{1}{\sqrt{N}} \sum_{\vec{q}} S_2(\vec{q}) e^{i\vec{q} \cdot \vec{X}(\vec{n})}, \quad (2.8a)$$

$$S_2(\vec{q}) = \frac{1}{\sqrt{N}} \sum_{\vec{n}} S_2(\vec{n}) e^{-i\vec{q} \cdot \vec{X}(\vec{n})}. \quad (2.8b)$$

Since the chains are rigid and form a two-dimensional array $\vec{\nu}$, $S_2(\vec{n}) \equiv S_2(n_1, \vec{\nu})$ is independent of n_1 , and hence $S_2(\vec{q})$ reduces to

$$S_2(0, \vec{q}_\perp) = \sqrt{N_1} \delta_{q_\xi 0} S_2(\vec{q}_\perp), \quad (2.9)$$

with

$$S_2(\vec{q}_\perp) = \frac{1}{\sqrt{N_c}} \sum_{\vec{\nu}} S_2(\vec{\nu}) e^{-i\vec{q}_\perp \cdot \vec{X}(\vec{\nu})}. \quad (2.10)$$

Here we have $\vec{X}(\vec{\nu}) = n_2 \vec{b} + n_3 \vec{c}$, and $\vec{q}_\perp = (q_\eta, q_\zeta)$, q_η, q_ζ being the components of \vec{q} along the orthorhombic axes. The interaction V^{RR} then reads

$$V_{QQ}^{RR} = \frac{N_1}{2} \sum_{\vec{q}_\perp} J_{QQ}(\vec{q}_\perp) S_2^\dagger(\vec{q}_\perp) S_2(\vec{q}_\perp), \quad (2.11)$$

$$J_{QQ}(\vec{q}_\perp) = 8J_a \cos\left(\frac{q_\eta b}{2}\right) \cos\left(\frac{q_\zeta c}{2}\right) + 2J_b \cos(q_\eta b). \quad (2.12)$$

In the following section we will derive explicit expressions for the quadrupolar interaction coefficients J_a, J_b and for the crystal field. The crystal field for the same configuration of neighboring interactions reads

$$V_{CF} = N_1 \sum_{\vec{\nu}} (8v_a + 2v_b) C_2(\vec{\nu}), \quad (2.13)$$

where the coefficients v_a and v_b are determined by Eq. (2.7). In the next section the theory will be applied to the study of van der Waals and electrostatic quadrupole interactions between C_{60} polymer chains.

III. DIRECT INTERCHAIN COUPLING

The orientation dependent interaction between two polymer chains in the $Immm$ crystal of AC_{60} is due to direct van der Waals interactions and to electric quadrupole forces between C_{60} monomers. The van der Waals interactions also determine the mutual chain orientations in polymerized C_{60} .

A. Direct van der Waals Interactions

Here we consider repulsive Born-Mayer and attractive London dispersion forces between interaction centers on monomers located in different chains. The interaction centers comprise C atoms and double bond- and single bond centers; they have been previously introduced for the description of the orientational disordered and ordered phases of C_{60} fullerite [32–34]. While in orientationally disordered C_{60} all C atoms are equivalent, this is no longer the case in the polymer phase and we have to take into account explicitly the geometrical constraints imposed by polymerization along the orthorhombic \vec{a} axis. Throughout this paper we assume polymer chains of symmetry D_{2h} . The neutron diffraction results of Ref. [14] show in fact that the symmetry of the chains in both KC_{60} and RbC_{60} is lower, C_{2h} . We attribute this reduction of symmetry to the molecular field of the originally ordered structures $Pmnn$ and $I2/m$. Since we start from an orientationally disordered structure $Immm$ and study the transition towards $Pmnn$ or $I2/m$, we keep the chain symmetry D_{2h} . It is convenient to classify the C atoms of a monomer in planar (100) sheets, perpendicular to \vec{a} (see Fig. 1). We label these sheets by an index $\lambda = 1, \dots, 17$. The position of sheet λ with respect to the center of mass of the monomer is determined by a vector $\vec{p}(\lambda)$:

$$\vec{p}(\lambda) = p(\lambda) \vec{e}_\xi, \quad (3.1)$$

with origin at the center of the monomer and end point at the intersection of sheet λ with the polymer axis. This intersection is called the center of the sheet. Here \vec{e}_ξ is a unit vector along the polymer axis. The atoms within sheet λ are labeled by an index $c(\lambda)$. We will use the notation $\Lambda = (\lambda, c(\lambda))$. The atomic positions relative to the center of mass of a monomer belonging to the polymer $\vec{\nu}$ which is rotated away from the standard orientation by the angle $\psi(\vec{\nu})$ then reads

$$\vec{r}(\Lambda, \psi(\vec{\nu})) = r(\lambda) \{ \cos[\phi(\Lambda) + \psi(\vec{\nu})] \vec{e}_\eta + \sin[\phi(\Lambda) + \psi(\vec{\nu})] \vec{e}_\zeta \} \quad (3.2)$$

with $r(\lambda) = d \sin \theta(\lambda)$. Here d is the radius of the C_{60} molecule, $\theta(\lambda)$ and $\phi(\Lambda)$ are respectively the polar and the azimuthal angle of the atom $c(\lambda)$ when the polymer is in the standard orientation. The position of atom Λ of the monomer at lattice site $\vec{n} = (n_1, \vec{\nu})$ is then given by

TABLE I. Lattice constants of the cubic and orthorhombic lattices of AC₆₀ and C₆₀ (units Å). Calculated direct interaction coefficients J for van der Waals and Coulomb interactions (units Kelvin), orthorhombic lattices.

	a_c	a_o	b_o	c_o	J_a^W	J_b^W	J_a^C	J_b^C
KC ₆₀	14.06	9.11	9.95	14.32	21.44	-6.61	10.70	-55.17
RbC ₆₀	14.08	9.14	10.11	14.23	21.33	-2.88	11.14	-50.56
CsC ₆₀	14.13	9.10	10.22	14.17	20.61	-1.50	11.65	-47.68
C ₆₀	14.15	9.14	9.90	14.66	13.13	-8.41	/	/

$$\vec{R}(\vec{n}, \Lambda, \psi(\vec{\nu})) = \vec{X}(\vec{n}) + \vec{\rho}(\Lambda, \psi(\vec{\nu})), \quad (3.3)$$

where $\vec{\rho}(\Lambda, \psi(\vec{\nu})) = \vec{p}(\lambda) + \vec{r}(\Lambda, \psi(\vec{\nu}))$. The distance between atoms Λ and Λ' belonging to monomers \vec{n} and \vec{n}' in different chains $\vec{\nu}$ and $\vec{\nu}'$ reads

$$\Delta(\vec{n}, \Lambda, \psi; \vec{n}', \Lambda', \psi') = |\vec{R}(\vec{n}, \Lambda, \psi) - \vec{R}(\vec{n}', \Lambda', \psi')|. \quad (3.4)$$

Here we have written ψ, ψ' for $\psi(\vec{\nu})$ and $\psi(\vec{\nu}')$ respectively. The van der Waals potential U^W between these atoms is then given by

$$U^W(\vec{n}, \Lambda, \psi; \vec{n}', \Lambda', \psi') = C_1 \exp(-C_2 \Delta) - B \Delta^{-6} \quad (3.5)$$

with Δ given by Eq. (3.4). Here C_1 and C_2 are the parameters of the repulsive Born-Mayer potential while B determines the strength of the van der Waals attraction (London dispersion forces). The interaction potential between monomers then reads

$$U^W(\vec{n}, \psi; \vec{n}', \psi') = \sum_{\Lambda, \Lambda'} U^W(\vec{n}, \Lambda, \psi; \vec{n}', \Lambda', \psi'), \quad (3.6)$$

where the double sum runs over the C atoms Λ, Λ' of the two monomers. In a similar way we can treat the potential due to interaction centers located on double bonds and single bonds of the monomers. For the case of three interaction centers between two C atoms participating in a double bond on the monomer, the present formulation leads to the consideration of 26 additional planar sheets, the inclusion of single bond centers adds 17 more sheets. Details of the van der Waals potentials between various types of interaction centers belonging to monomers on different chains are given in Appendix B. As a result the potential between two monomers is again expressed by Eq. (3.6), where now the indices Λ and Λ' run over atoms, double bond- and single bond interaction centers. Having determined $U^W(\vec{n}, \psi; \vec{n}', \psi')$, we proceed as in Sect. II, Eqs. (2.3)-(2.12). As a result we obtain the van der Waals contributions J_a^W and J_b^W to the quadrupolar interactions J_a and J_b . Numerical results are found in Table I. There we quote the interchain van der Waals interaction coefficients for orthorhombic lattice constants a_o, b_o, c_o of polymerized AC₆₀, A=K, Rb, Cs and polymerized C₆₀. Similarly we determine the crystal field coefficients v_a^W and v_b^W . The results are quoted in Table II.

TABLE II. Crystal field coefficients due to neighboring chains v_a^W etc., units K.

	v_a^W	v_b^W	v_a^C	v_b^C
KC ₆₀	24.24	-73.06	-99.12	422.53
RbC ₆₀	23.44	-15.31	-92.99	400.99
CsC ₆₀	21.49	5.57	-89.55	387.06
C ₆₀	24.45	-101.01	/	/

B. Electrostatic Quadrupolar Interactions

The charge transfer of one electron from the alkali atom to the C₆₀ molecule leads to an occupation of the lowest unoccupied molecular orbital (LUMO) levels which are of T_{1u} symmetry [35]. Thereby the crystal field of the C₆₀⁻ ion acquires an electronic component that favors the same orientation of the neighboring molecules along [110] such that the stereospecific cycloaddition occurs [19]. We have studied the electronic charge distribution on the C₆₀⁻ units in the polymer chain by using a tight binding model [21]. The charge is mainly concentrated in the equatorial region of C₆₀⁻, in agreement with NMR results [36]. We find that only even l multipoles are allowed; in particular each C₆₀ unit has an electric quadrupole. In the following we adopt a simple model of charge distribution. By using the labeling of C atoms of [36], we locate a charge of -0.12 (units electron charge $|e|$) on each bond C15-C16. These charges are fixed at a distance $d = 3.52$ Å from the center of the C₆₀⁻ ball. In the center we put a charge -0.76 . The position of these three charges on a C₆₀⁻ monomer centered at the lattice site $\vec{n} = (n_1, \vec{\nu})$ belonging to chain $\vec{\nu}$ is then given by

$$\vec{R}(\vec{n}, \alpha, \psi(\vec{\nu})) = \vec{X}(\vec{n}) + \vec{D}(\alpha, \psi(\vec{\nu})), \quad (3.7)$$

where

$$\vec{D}(\alpha, \psi(\vec{\nu})) = d(\alpha) [\vec{e}_\eta \cos \psi(\vec{\nu}) + \vec{e}_\zeta \sin \psi(\vec{\nu})], \quad (3.8)$$

where $d(\alpha) = \pm d$ for $\alpha = 1, 2$ corresponding to the two charges $Q_\alpha = -0.12$ and $d(\alpha) = 0$ for $\alpha = 3$, corresponding to the central charge $Q_\alpha = -0.76$. The distance between two charges belonging to two monomers on different chains is then given by

$$\Delta(\vec{n}, \alpha, \psi; \vec{n}', \alpha', \psi') = |\vec{R}(\vec{n}, \alpha, \psi) - \vec{R}(\vec{n}', \alpha', \psi')|, \quad (3.9)$$

where ψ, ψ' stands for $\psi(\vec{\nu}), \psi(\vec{\nu}')$. The Coulomb interaction between these two monomers then reads

$$U^C(\vec{n}, \psi; \vec{n}', \psi') = \sum_{i, i'} F \frac{Q_i Q_{i'}}{\Delta(\vec{n}, \alpha, \psi; \vec{n}', \alpha', \psi')}. \quad (3.10)$$

With our units of charges and with lengths in Å, with $F = 167000$ K Å, the energy U^C is measured in units Kelvin. One now proceeds as before with U^W . We take

into account the same configuration of neighbors as before, sum over all chains in the crystal, expand the total potential in terms of SARFs and obtain the interaction coefficients J_a^C, J_b^C for the electrostatic quadrupole-quadrupole interaction and the coefficients v_a^C and v_b^C for the electrostatic crystal field. The results are also quoted in Table I and Table II respectively. Adding the quadrupole-quadrupole contributions from the van der Waals and the electrostatic interchain potentials we obtain the total quadrupolar interaction V_{QQ}^{RR} , expression (2.11), where $J_{QQ}(\vec{q}_\perp)$ is given by Eq. (2.12) with

$$J_a = J_a^W + J_a^C, \quad (3.11a)$$

$$J_b = J_b^W + J_b^C. \quad (3.11b)$$

Notice that for polymerized pristine C_{60} , there is no electrostatic quadrupole due to charge transfer, and hence J_a^C and J_b^C are zero. We observe that in principle the deformation of the monomer in C_{60} from $I_h \rightarrow D_{2h}$ leads to a redistribution of the electric charge on the neutral molecule. Here it is assumed that these effects are included in J_a^W and J_b^W .

We return to the quadrupolar interaction $J(\vec{q})$ and study its wave number dependence. In two-dimensional \vec{q}_\perp space (q_η, q_ζ) we have at the Brillouin zone (BZ) center $\vec{q}_\perp = (0, 0) = \vec{q}_\Gamma$

$$J_{QQ}(\vec{q}_\Gamma) = 8J_a + 2J_b. \quad (3.12)$$

With the numerical values of Table I we conclude that for polymerized AC_{60} , $A=K, Rb, Cs$ as well as for polymerized C_{60} , $J(\vec{q}_\Gamma) > 0$. On the other hand, at the Brillouin zone boundary $\vec{q}_\perp = (0, \frac{2\pi}{c}) = \vec{q}_Z$ we get

$$J_{QQ}(\vec{q}_Z) = -8J_a + 2J_b, \quad (3.13)$$

with $J(\vec{q}_Z) < 0$ and $|J(\vec{q}_Z)| > J(\vec{q}_\Gamma)$. The dominance and negative sign of $J(\vec{q}_Z)$ leads to a condensation of $S_2(\vec{q})$ at $\vec{q}_\perp = \vec{q}_Z$:

$$\langle S_2(\vec{q}_\perp) \rangle = \sqrt{N_c} \sigma \delta_{\vec{q}_\perp, \vec{q}_Z}, \quad (3.14)$$

which is the condensation scheme proposed earlier [18]. Here $\langle \rangle$ stands for a thermal average over the crystal, σ is the order parameter amplitude. The number of chains N_c corresponds to the number of lattice points in the orthorhombic (\vec{b}, \vec{c}) plane. Condensation at \vec{q}_Z implies that the chains in the same basal plane (\vec{a}, \vec{b}) of the orthorhombic lattice all have the same orientation, but the orientation alternates in neighboring planes at distance $c/2$. This is the ‘‘antiferrotational’’ structure $Pmnn$ (Fig. 1a). We find that the rotation-rotation interaction due to van der Waals forces and electrostatic quadrupolar forces leads to $Pmnn$ for KC_{60} , RbC_{60} and CsC_{60} , irrespective of the orthorhombic lattice constants. While for KC_{60} this structure has been found by experiment [7,12], the experimental result for RbC_{60} [12,14] and CsC_{60} [13] is $I2/m$. We conclude that the alkalis must play a specific role and we will investigate this problem in the next section.

On the other hand, for polymerized pristine C_{60} , our analysis confirms the experimental result $Pmnn$ [22,23].

IV. ALKALI-MEDIATED INTERACTIONS

A. Translation-Rotation Coupling

In orientationally disordered molecular crystals or in crystals containing ions with orientational disorder, the coupling of molecular rotations with center of mass lattice displacements of molecules and of surrounding ions plays an important role in determining the structural properties. For a review on the so-called translation-rotation (TR) coupling, see Ref. [37]. Here we will study the corresponding coupling of the rotational motion of polymer chains with the lattice displacements of the surrounding alkali ions. We extend the model of an orthorhombic crystal consisting of orientationally disordered rigid polymers with axis of polymerization along the orthorhombic ξ direction (Sect. II) by including the alkali metal ions at equilibrium lattice positions

$$\vec{X}(\vec{n}_A) = n_{A1}\vec{a} + n_{A2}\vec{b} + n_{A3}\vec{c}, \quad (4.1)$$

where $\vec{n}_A = (n_{A1}, n_{A2}, n_{A3})$ are the lattice indices of the alkali atoms. For a C_{60}^- monomer at lattice site $\vec{n} = (n_1, n_2, n_3)$, the six nearest neighbor alkalis are located at $(n_1 \pm \frac{1}{2}, n_2 \pm \frac{1}{2}, n_3)$, $(n_1, n_2, n_3 \pm \frac{1}{2})$. Taking into account lattice displacements $\vec{u}_A(\vec{n}_A)$ we write for the actual positions of the alkalis

$$\vec{R}(\vec{n}_A) = \vec{X}(\vec{n}_A) + \vec{u}_A(\vec{n}_A). \quad (4.2)$$

The distance between a C atom in position Λ belonging to a C_{60}^- monomer at lattice site $\vec{n} = (n_1, \vec{\nu})$ in the polymer chain $\vec{\nu}$ and a surrounding alkali ion at \vec{n}_A is given by $|\vec{R}(\vec{n}, \Lambda, \psi(\vec{\nu})) - \vec{R}(\vec{n}_A)|$ or equivalently by

$$\Delta(\vec{n}, \Lambda, \psi(\vec{\nu}); \vec{n}_A) = |\vec{\rho}(\Lambda, \psi(\vec{\nu})) + \vec{X}(\vec{n} - \vec{n}_A) - \vec{u}_A(\vec{n}_A)|. \quad (4.3)$$

Here we have used expression (3.3) for $\vec{R}(\vec{n}, \Lambda, \psi(\vec{\nu}))$, $\psi(\vec{\nu})$ being the orientation angle of the polymer chain. The van der Waals interaction of the monomer and the alkali ion is then given by

$$U^W(\vec{n}, \psi(\vec{\nu}); \vec{n}_A) = \sum_{\Lambda} C_1 \exp(-C_2 \Delta) - B \Delta^{-6}, \quad (4.4)$$

where the potential parameters C_1, C_2 and B refer to the C-A interaction (see Appendix B). The Coulomb interaction potential of the quadrupolar electric charges Q_α on the C_{60}^- monomers (See Sect. III B) with an alkali ion A^+ with unit charge Q^A reads:

$$U^C(\vec{n}, \psi(\vec{\nu}); \vec{n}_A) = F \sum_{\alpha} \frac{Q_\alpha Q^A}{\Delta(\vec{n}, \alpha, \Lambda, \psi(\vec{\nu}); \vec{n}_A)} \quad (4.5a)$$

where

$$\begin{aligned} & \Delta(\vec{n}, \alpha, \Lambda, \psi(\vec{\nu}); \vec{n}_A) \\ & = |\vec{D}(i, \psi(\vec{\nu})) + \vec{X}(\vec{n} - \vec{n}_A) - \vec{u}_A(\vec{n}_A)| \end{aligned} \quad (4.5b)$$

is the distance between the charge α on the monomer and the center of the alkali ion. Assuming that the lattice displacements are small (in comparison to the lattice constants), we expand these potentials (U stands for U^W or U^C) in terms of \vec{u}_A and retain the first two terms:

$$\begin{aligned} U(\vec{n}, \psi(\vec{\nu}); \vec{n}_A) & = U^{(0)}(\vec{n} - \vec{n}_A, \psi(\vec{\nu})) \\ & + \sum_i U_i^{(1)}(\vec{n} - \vec{n}_A, \psi(\vec{\nu})) u_{Ai}(\vec{n}_A), \end{aligned} \quad (4.6)$$

where i labels the Cartesian components along the orthorhombic axes. The first term on the right hand side (RHS) corresponds to the situation $\vec{u}_A = \vec{0}$, the alkali ion is at its equilibrium position. Exploiting the angular dependence of $U^{(0)}$ we expand it in terms of SARFs. Since each monomer is located at a center of symmetry with respect to the surrounding alkalis in the orthorhombic lattice, only $C_l(\psi(\vec{\nu}))$ terms contribute to

$$\sum_{\vec{n}_A} U^{(0)}(\vec{n} - \vec{n}_A, \psi(\vec{\nu})) = \sum_{\vec{n}_A} v^{(0)}(\vec{n}_A - \vec{n}) C_2(\psi(\vec{\nu})), \quad (4.7)$$

where

$$v^{(0)}(\vec{n}_A - \vec{n}) = \frac{1}{\pi} \int_0^{2\pi} d\psi(\vec{\nu}) U^{(0)}(\vec{n} - \vec{n}_A, \psi(\vec{\nu})) C_2(\psi(\vec{\nu})). \quad (4.8)$$

Here we restrict ourselves to the lowest order multipoles with $l = 2$. Expression (4.7) stands for the interaction of one monomer at site n_1 in chain $\vec{\nu}$ with six surrounding alkali atoms at equilibrium lattice sites $\vec{X}(\vec{n}_A)$. Since all monomers of the chain are equivalent, the RHS result does not depend on n_1 . Taking into account U^C and U^W and summing over all monomer sites, we obtain the crystal field potential due to the nearest neighbor alkali atoms

$$V_{CF}^A = N_1 \sum_{\vec{\nu}} (4v_{ab}^A + 2v_c^A) C_2(\psi(\vec{\nu})) \quad (4.9)$$

where we have

$$v_{ab}^A = v_{ab}^{A,W} + v_{ab}^{A,C}, \quad (4.10a)$$

$$v_c^A = v_c^{A,W} + v_c^{A,C}. \quad (4.10b)$$

Here v_{ab} and v_c refer to alkalis located at $(\pm\frac{1}{2}, \pm\frac{1}{2}, 0)$ and $(0, 0, \pm\frac{1}{2})$ respectively, counted from the monomer center \vec{n} . Numerical values of these coefficients are quoted in Table III.

TABLE III. Crystal field coefficients due to alkalis, units K.

	$v_{ab}^{A,W}$	$v_c^{A,W}$	$v_{ab}^{A,C}$	$v_c^{A,C}$
KC ₆₀	-10.55	16.38	-497.98	1137.42
RbC ₆₀	-14.30	26.44	-493.28	1161.03
CsC ₆₀	-19.91	30.44	-497.81	1177.16

The second term on the RHS of Eq. (4.6) is the proper TR contribution, $U_i^{(1)}$ stands for the first order derivative of U with respect to u_{Ai} . Expanding $U_i^{(1)}$ in terms of SARFs, summing over the surrounding six alkalis of the monomer and exploiting the symmetry of the orthorhombic lattice, we find in lowest order $l = 2$ of the multipole expansion:

$$\begin{aligned} & \sum_{\vec{n}_A} U_i^{(1)}(\vec{n} - \vec{n}_A, \psi(\vec{\nu})) u_{Ai}(\vec{n}_A) \\ & = \sum_{\vec{n}_A} v_i^{(1)}(\vec{n}_A - \vec{n}) S_2(\psi(\vec{\nu})) u_{Ai}(\vec{n}_A). \end{aligned} \quad (4.11)$$

Here we retain only the terms containing the function S_2 and drop those with C_2 . Indeed it can be shown that TR terms with C_2 do not contribute to a change of the orthorhombic lattice structure. The coefficients $v_i^{(1)}(\vec{n}_A - \vec{n})$ are obtained by

$$v_i^{(1)}(\vec{n}_A - \vec{n}) = \frac{1}{\pi} \int_0^{2\pi} d\psi(\vec{\nu}) U_i^{(1)}(\vec{n} - \vec{n}_A, \psi(\vec{\nu})) S_2(\psi(\vec{\nu})). \quad (4.12)$$

Summing over all monomers in the crystal, the total TR potential due to $U^W + U^C$ is found to be

$$V^{TR} = \sum_{\vec{n}} \sum_{\vec{n}_A} \sum_i v_i^{(1)}(\vec{n}_A - \vec{n}) S_2(\psi(\vec{\nu})) u_{Ai}(\vec{n}_A). \quad (4.13)$$

We mention the symmetry property

$$v_i^{(1)}(\vec{n}_A - \vec{n}) = -v_i^{(1)}(\vec{n} - \vec{n}_A). \quad (4.14)$$

From expression (4.12) it follows that all six coefficients $v_1^{(1)}(\vec{n}_A - \vec{n})$ are zero. The only nonzero coefficients are $v_2^{(1)}(0, 0, \pm\frac{1}{2}) = \mp v_{2,c}^A$, $v_3^{(1)}(\pm\frac{1}{2}, \pm\frac{1}{2}, 0) = \mp v_{3,ab}^A$ and $v_3^{(1)}(\pm\frac{1}{2}, \mp\frac{1}{2}, 0) = \mp v_{3,ab}^A$, where

$$v_{2,c}^A = v_{2,c}^{A,W} + v_{2,c}^{A,C}, \quad (4.15a)$$

$$v_{3,ab}^A = v_{3,ab}^{A,W} + v_{3,ab}^{A,C}. \quad (4.15b)$$

Numerical values are given in Table IV. We define Fourier transforms of displacements by

$$\vec{u}_A(\vec{n}_A) = \frac{1}{\sqrt{Nm_A}} \sum_{\vec{q}} e^{i\vec{q} \cdot \vec{X}(\vec{n}_A)} \vec{u}_A(\vec{q}), \quad (4.16a)$$

$$\vec{u}_A(\vec{q}) = \sqrt{\frac{m_A}{N}} \sum_{\vec{n}_A} e^{-i\vec{q} \cdot \vec{X}(\vec{n}_A)} \vec{u}_A(\vec{n}_A). \quad (4.16b)$$

TABLE IV. Calculated indirect interactions coefficients for TR coupling (v in units K/Å). Electronic polarizability parameters, d_A in units Å, g_A and calculated λ_b , λ_c in units K.

	$v_{2,c}^{A,W}$	$v_{3,ab}^{A,W}$	$v_{2,c}^{A,C}$	$v_{3,ab}^{A,C}$	d_A	λ_b	λ_c	g_A
KC ₆₀	4.57	4.24	317.71	199.98	1.47	9.28	51.20	43.25
RbC ₆₀	7.48	5.70	326.36	195.17	1.82	13.25	83.52	35.00
CsC ₆₀	8.59	7.79	332.29	194.84	1.87	14.27	90.75	34.00

Using in addition Eq. (2.10), we rewrite Eq. (4.13):

$$V^{TR} = \sqrt{\frac{N_1}{m_A}} \sum_{\vec{q}_\perp} \sum_i v_i^{(1)}(\vec{q}_\perp) S_2^\dagger(\vec{q}_\perp) u_{Ai}(0, \vec{q}_\perp), \quad (4.17)$$

where

$$v_i^{(1)}(\vec{q}_\perp) = i \sum_{\vec{n}_A} v_i^{(1)}(\vec{n}_A - \vec{n}) \sin(\vec{q} \cdot \vec{X}(\vec{n}_A - \vec{n})), \quad (4.18)$$

or equivalently

$$\vec{v}^{(1)}(\vec{q}_\perp) = \begin{pmatrix} 0 \\ -2iv_{2,c}^A \sin(q_\zeta \frac{c}{2}) \\ -4iv_{3,ab}^A \sin(q_\eta \frac{b}{2}) \end{pmatrix}. \quad (4.19)$$

We see that the rotational motion of the chains about the \vec{a} axis induces displacements of the alkali atoms only along the \vec{b} and \vec{c} axes. We observe that the coupling $v_i^{(1)}(\vec{q}_\perp)$ vanishes at $\vec{q}_\perp = \vec{q}_Z$.

In order to relate our results to elastic deformations of the lattice, we consider the RHS of Eq. (4.17) in the long wavelength regime and transform to acoustic (ac) lattice displacements

$$\vec{s}(\vec{q}) = \sqrt{\frac{m_A}{m}} \vec{u}_A(\vec{q}) + \sqrt{\frac{m_{C_{60}}}{m}} \vec{u}_{C_{60}}(\vec{q}), \quad (4.20)$$

where $m = m_A + m_{C_{60}}$ is the total mass per primitive unit cell, $m_{C_{60}}$ being the mass of a C₆₀ monomer. The acoustic part of V^{TR} then reads

$$V_{ac}^{TR} = \sqrt{N_1} \sum_{\vec{q}_\perp} \sum_i \hat{v}_i^{(1)}(\vec{q}_\perp) s_i(0, \vec{q}_\perp) S_2^\dagger(\vec{q}_\perp). \quad (4.21)$$

The sum over i is now restricted to the components η and ζ and hence

$$\vec{v}_{ac}^{(1)}(\vec{q}_\perp) = -\frac{i}{\sqrt{m}} \begin{pmatrix} cq_\zeta v_{2,c}^A \\ 2bq_\eta v_{3,ab}^A \end{pmatrix}. \quad (4.22)$$

The translational part of the acoustic lattice energy is given by

$$V_{ac}^{TT} = \frac{1}{2} \sum_{\vec{q}} \sum_{i,j} s_i^\dagger(\vec{q}) M_{ij}(\vec{q}) s_j(\vec{q}). \quad (4.23)$$

Here $M_{ij}(\vec{q})$ is the dynamical matrix of the orthorhombic crystal in absence of TR coupling. In the following

TABLE V. Interactions at $\vec{q}_\perp = \vec{q}_\Gamma$, units K.

	$J_{QQ}^C(\vec{q}_\Gamma)$	$J_{QQ}^W(\vec{q}_\Gamma)$	$-J_{ac}(\vec{q}_\Gamma)$	$-J_{ep}(\vec{q}_\Gamma)$	$J(\vec{q}_\Gamma)$
KC ₆₀	-24.80	158.30	-37.72	-225.02	-129.24
RbC ₆₀	-12.03	164.88	-39.44	-691.62	-578.21
CsC ₆₀	-2.18	161.88	-40.65	-837.14	-718.09
C ₆₀	/	88.22	/	/	88.22

we need only to retain the components (η, ζ) of $\vec{s}(0, \vec{q}_\perp)$. Then $M(\vec{q})$ reduces to a 2×2 matrix:

$$M(\vec{q}_\perp) = \frac{1}{\rho} \begin{pmatrix} q_\eta^2 c_{22} + q_\zeta^2 c_{44} & q_\eta q_\zeta (c_{23} + c_{44}) \\ q_\eta q_\zeta (c_{23} + c_{44}) & q_\zeta^2 c_{33} + q_\eta^2 c_{44} \end{pmatrix}. \quad (4.24)$$

Here ρ is the mass density in the body centered orthorhombic unit cell, $\rho = 2m/(abc)$. We use the Voigt notation for the orthorhombic elastic constants c_{22} etc.. We now consider

$$V_{ac} = V_{ac}^{TR} + V_{ac}^{TT}. \quad (4.25)$$

For a fixed configuration of orientations $\{S_2(\vec{q}_\perp)\}$, we minimize V_{ac} with respect to $s_i(0, \vec{q}_\perp)$, $i = \eta, \zeta$, and obtain

$$s^\dagger(0, \vec{q}_\perp) = -\sqrt{N_1} M^{-1}(\vec{q}_\perp) \vec{v}^{(1)}(\vec{q}_\perp) S_2^\dagger(\vec{q}_\perp). \quad (4.26)$$

Substitution of this expression into V_{ac} leads to the effective rotation-rotation interaction which we denote by V_{ac}^{RR} :

$$V_{ac}^{RR} = -\frac{N_1}{2} \sum_{\vec{q}_\perp} S_2^\dagger(\vec{q}_\perp) J_{ac}(\vec{q}_\perp) S_2(\vec{q}_\perp), \quad (4.27)$$

where

$$J_{ac}(\vec{q}_\perp) = \vec{v}_{ac}^{(1)\dagger}(\vec{q}_\perp) M^{-1}(\vec{q}_\perp) \vec{v}_{ac}^{(1)}(\vec{q}_\perp). \quad (4.28)$$

Since $J_{ac}(\vec{q}_\perp) > 0$, the lattice mediated interaction V_{ac}^{RR} is always attractive. The largest value is obtained for $\vec{q}_\perp = \vec{q}_\Gamma = \vec{0}$:

$$\lim_{q_\zeta \rightarrow 0} J_{ac}(\vec{q}_\perp)|_{q_\eta=0} = \frac{2(v_{2,c}^A)^2 c}{c_{44} ab} \equiv J_{ac}(\vec{q}_\Gamma). \quad (4.29)$$

With $c_{44} = 870 \text{ K } \text{Å}^{-3}$ taken from Ref. [38] for C₆₀-fullerite, and the values of $v_{2,c}^A$ from Table IV, we find $J_{ac}(\vec{q}_\Gamma)$ as quoted in Table V for KC₆₀, RbC₆₀ and CsC₆₀. The attractive interaction at \vec{q}_Γ favors a condensation of a ferrorotational structure where all polymer chains have the same orientation, i. e. the space group $I2/m$. However comparison of the numerical values of $J_{ac}(\vec{q}_\Gamma)$ and $J(\vec{q}_Z)$ shows that the interaction, which leads to the anti-ferrorotational structure $Pmnn$, is dominant. Hence the TR coupling mechanism is not sufficient to explain the structural difference between KC₆₀ and Cs-, RbC₆₀. In part IV B we will exploit a different alkali-mediated interaction mechanism. It is based on a specific *quadrupolar* electronic polarizability of the alkali ions.

B. Quadrupolar Polarizability

We will now include the role of the specific electronic polarizability of the alkali ions. It is known from work on the ammonium halides [39] that the indirect interaction of two NH_4^+ tetrahedra via the polarizable halide ions plays an essential role in determining the various crystalline phases of the ammonium halides NH_4X , $\text{X} = \text{Cl}, \text{Br}$ and I . However, in the present problem, since the C_{60} monomers have symmetry D_{2h} , they do not couple to the dipolar electronic polarizability of the alkali metal ions. We have to resort to the quadrupolar polarizability. Since the C_{60}^- units in a polymer chain are rigidly linked in the same orientation, the C_{60}^- chains, which support electric quadrupoles, produce coherent electric field gradients which induce an anisotropic (quadrupolar) deformation of the residual electronic charge of the alkalis. The presence of residual electronic charge is seen as a consequence of the uniquely large interstitial space between the C_{60} molecules (we recall that in AC_{60} , the A^+ cations occupy the formerly octahedral positions of the cubic phase). Within a touching sphere model, with 5 Å as the effective van der Waals radius of the C_{60} molecule [40] and a cubic lattice constant $a = 14.15$ Å, we estimate the radius of the interstitial sphere to be $R_A \approx 2.075$ Å. Although the charge transfer from the alkali atom to the C_{60} molecule is considered as complete, there still will be a charge of $0.1 - 0.15|e|$ left inside the interstitial sphere centered at each alkali site. In Appendix C we discuss in more detail the microscopic origin of the quadrupolar polarizability of the cations. Within a tight-binding model of the conduction electron band, we expand the electron wave function at an alkali site in terms of local s and d functions. If there is an appreciable weight of d -states, then the alkalis acquire a quadrupolar moment. We model the corresponding charge distribution of each alkali ion by a symmetric linear dumbbell centered on lines along the \vec{a} direction. We take dumbbells with equal charges $Q_\beta = q_A$, $\beta = 1, 2$, at distances $\pm d_A$ from the center. The numerical values of d_A (Table IV) are the average radii of valence electron d shells calculated with atomic wave functions $3d_{3/2}$, $4d_{3/2}$ and $5d_{3/2}$ for K^+ , Rb^+ and Cs^+ respectively (Appendix C). We observe that the d_A values for Cs^+ and Rb^+ are close to each other but differ from K^+ . We consider d shells because they can support an electric quadrupole moment. On a same crystalline line along \vec{a} , these dumbbells are parallel with their axis perpendicular to \vec{a} and a same orientation angle ψ with the \vec{c} axis. In the crystal we then have chains of alkali dumbbells, where the rigid chain is not imposed by intrachain interactions (as is the case for the C_{60} polymers formed by cycloaddition) but by the surrounding C_{60}^- chains. The location of a dumbbell in the crystal is determined by $\vec{n}_A = (n_{A1}, \vec{v}_A)$, where $\vec{v}_A = (n_{2A}, n_{3A})$ denotes the chain and where n_{A1} labels the dumbbell within the chain. The orientational motion of an alkali dumbbell is characterized by SARFs

$s_2(\vec{v}_A) = \sin(2\psi(\vec{v}_A))$, independent of n_{A1} . The electric quadrupole-quadrupole interaction potential between a C_{60} monomer at \vec{n} and a surrounding alkali dumbbell at \vec{n}_A is given by

$$U^{QQ}(\vec{n}, \psi(\vec{v}); \vec{n}_A, \psi(\vec{v}_A)) = F \sum_{\alpha, \beta} \frac{Q_\alpha Q_\beta}{\Delta(\vec{n}, \alpha, \psi(\vec{v}); \vec{n}_A, \beta, \psi(\vec{v}_A))} \quad (4.30)$$

where

$$\Delta(\vec{n}, \alpha, \psi(\vec{v}); \vec{n}_A, \beta, \psi(\vec{v}_A)) = |\vec{D}(\alpha, \psi(\vec{v})) + \vec{X}(\vec{n} - \vec{n}_A) - \vec{d}_A(\beta, \psi(\vec{v}_A))| \quad (4.31)$$

is the distance between a charge Q_α on the monomer and a charge Q_β on the alkali dumbbell. The position of the charge β on the dumbbell \vec{n}_A in the crystal reads

$$\vec{X}(\vec{n}_A, \beta) = \vec{X}(\vec{n}_A) + \vec{d}_A(\beta, \psi(\vec{v}_A)), \quad (4.32)$$

where \vec{d}_A is the position vector of the charge with respect to the center of the dumbbell. Explicitly we have

$$\vec{d}_A(\beta, \psi(\vec{v}_A)) = \pm d_A \{ \cos[\psi(\vec{v}_A)] \vec{e}_\eta + \sin[\psi(\vec{v}_A)] \vec{e}_\zeta \}, \quad (4.33)$$

where $+$ and $-$ refer to the two quadrupolar charges.

The potential (4.30) is expanded in SARFs. After summation over the polymer chains \vec{n} and the surrounding alkalis \vec{n}_A we find (compare with Eq. (2.5a)):

$$V^{Ss} = \sum_{n_1, n_{A1}} \sum_{\vec{v}, \vec{v}_A} \lambda(n_1, \vec{v}; n_{A1}, \vec{v}_A) S_2(\vec{v}) s_2(\vec{v}_A), \quad (4.34)$$

where

$$\lambda(n_1, \vec{v}; n_{A1}, \vec{v}_A) = \frac{1}{\pi^2} \int_0^{2\pi} d\psi(\vec{v}) \int_0^{2\pi} d\psi(\vec{v}_A) \times U^{QQ}(\vec{n}, \psi(\vec{v}); \vec{n}_A, \psi(\vec{v}_A)) S_2(\psi(\vec{v})) s_2(\vec{v}_A). \quad (4.35)$$

Going over to Fourier space we have

$$V^{Ss} = N_1 \sum_{\vec{q}_\perp} \lambda(\vec{q}_\perp) S_2^\dagger(\vec{q}_\perp) s_2(\vec{q}_\perp), \quad (4.36)$$

where

$$\lambda(\vec{q}_\perp) = 4\lambda_b \cos\left(\frac{q_\eta b}{2}\right) + 2\lambda_c \cos\left(\frac{q_\zeta c}{2}\right). \quad (4.37)$$

Here we have restricted ourselves to the six nearest neighbors \vec{n}_A of a given monomer \vec{n} . With the values d_A of Table IV and with the same value $q_A = 0.12$ for the three compounds, we have calculated the interaction energies λ_b and λ_c quoted in Table IV. The quantity $|\lambda(\vec{q}_\perp)|$ is maximum at $\vec{q}_\perp = \vec{q}_\Gamma$ in contradistinction with the direct RR interaction $J_{QQ}(\vec{q}_\perp)$, Eq. (2.12). The intraionic

restoring forces of the electronic shells of the cations are described by a sum of single particle energy terms

$$V^{ss} = g_A \sum_{\vec{n}_A} s_2^2(\vec{n}_A) = N_1 g_A \sum_{\vec{q}_\perp} s_2^\dagger(\vec{q}_\perp) s_2(\vec{q}_\perp), \quad (4.38)$$

with $g_A > 0$. The self-energy g_A is inversely proportional to the quadrupolar electronic polarizability and hence $g_{Cs} < g_{Rb} < g_K$ (see Table IV). These concepts are inspired from the shell model of lattice dynamics where anisotropic electronic polarizabilities have been introduced [41]. The direct interchain coupling of alkali quadrupoles is numerically small and will be neglected. We now consider the sum

$$V_{ep}^{RR} = V^{Ss} + V^{ss}, \quad (4.39)$$

where the subscript ep refers to the quadrupolar electronic polarizability of the cations. We assume that the induced cation quadrupoles follow adiabatically the motion of the C_{60}^- chains. For a given configuration $\{S_2(\vec{q}_\perp)\}$ of the latter, we minimize V_s^{RR} with respect to $s_2(\vec{q}_\perp)$ and find

$$s_2(\vec{q}_\perp) = -\frac{1}{2} \frac{\lambda(\vec{q}_\perp)}{g_A} S_2(\vec{q}_\perp). \quad (4.40)$$

Substitution into V_{ep}^{RR} leads to the cation quadrupolar electronic polarizability mediated rotational interaction

$$V_{ep}^{RR} = -\frac{1}{2} N_1 \sum_{\vec{q}_\perp} J_{ep}(\vec{q}_\perp) S_2^\dagger(\vec{q}_\perp) S_2(\vec{q}_\perp), \quad (4.41)$$

where

$$J_{ep}(\vec{q}_\perp) = \frac{1}{2} \frac{\lambda^2(\vec{q}_\perp)}{g_A}. \quad (4.42)$$

This interaction is always attractive and maximum in absolute value at $\vec{q}_\perp = \vec{q}_\Gamma$ (as is the case for the lattice mediated interaction V_{ac}^{RR}). Both V_{ep}^{RR} and V_{ac}^{RR} lead to a condensation of $S_2(\vec{q}_\perp)$ at \vec{q}_Γ and hence to the ferro-rotational structure $I2/m$:

$$\langle S_2(\vec{q}_\perp) \rangle = \sqrt{N_c} \sigma \delta_{\vec{q}_\perp, \vec{q}_\Gamma}, \quad (4.43)$$

where σ is the order parameter amplitude.

In the following section we will discuss the competition between the direct rotational interaction of C_{60} chains and the indirect, alkali mediated interaction.

V. STABILITY OF STRUCTURES

The orientational quadrupolar interaction V^{RR} between C_{60} chains is the sum of the direct interchain potential V_{QQ}^{RR} , Eq. (2.11) and of the indirect, alkali-mediated potentials V_{ac}^{RR} , Eq. (4.27), and V_{ep}^{RR} , Eq. (4.41). Hence we write

TABLE VI. Interactions at $\vec{q}_\perp = \vec{q}_Z$, units K.

	$J_{QQ}^C(\vec{q}_Z)$	$J_{QQ}^W(\vec{q}_Z)$	$-J_{ac}(\vec{q}_Z)$	$-J_{ep}(\vec{q}_Z)$	$J(\vec{q}_Z)$
KC ₆₀	-195.84	-184.70	0	-49.26	-429.80
RbC ₆₀	-190.21	-176.40	0	-185.80	-552.41
CsC ₆₀	-188.54	-167.88	0	-227.64	-584.05
C ₆₀	/	-121.86	/	/	-121.86

$$V^{RR} = V_{QQ}^{RR} + V_{ac}^{RR} + V_{ep}^{RR}, \quad (5.1)$$

or equivalently

$$V^{RR} = \frac{N_1}{2} \sum_{\vec{q}_\perp} J(\vec{q}_\perp) S_2^\dagger(\vec{q}_\perp) S_2 \vec{q}_\perp, \quad (5.2)$$

with

$$J(\vec{q}_\perp) = J_{QQ}(\vec{q}_\perp) - J_{ac}(\vec{q}_\perp) - J_{ep}(\vec{q}_\perp). \quad (5.3)$$

Here the direct interaction $J_{QQ}(\vec{q}_\perp)$, due to van der Waals and Coulomb quadrupole-quadrupole potentials, is given by Eq. (2.12), with J_a and J_b defined in Eqs. (3.11a), (3.11b). The acoustic lattice displacements mediated interaction $J_{ac}(\vec{q}_\perp)$ is given by Eq. (4.28) while the electronic polarizability mediated interaction $J_{ep}(\vec{q}_\perp)$ is defined by Eq. (4.42). We have already shown that the direct interaction $J_{QQ}(\vec{q}_\perp)$ becomes maximum and attractive at the Brillouin zone boundary $\vec{q}_\perp = \vec{q}_Z$, and hence favors the antiferro-rotational structure $Pmnn$. On the other hand the alkali mediated interactions $J_{ac}(\vec{q}_\perp)$ and $J_{ep}(\vec{q}_\perp)$ both are attractive and maximum at the Brillouin zone center $\vec{q}_\perp = \vec{q}_\Gamma$, and hence favor the ferro-rotational structure $I2/m$. The strength of the indirect interactions depends on the specific nature of the alkali ions.

We first consider $J(\vec{q}_\Gamma)$. From Eqs. (3.12), (4.29) and (4.42) we find the numerical values quoted in Table V.

Next we calculate $J(\vec{q}_Z)$. The results are quoted in Table VI. We have taken into account that there is no coupling to acoustic phonons at \vec{q}_Z . In Fig. 3 we have plotted the total rotational interaction $J(\vec{q}_\perp)$ as a function of q_ζ along the line $\vec{q}_\Gamma - \vec{q}_Z$. In Eq. (5.3) we have used for $J_{ac}(\vec{q}_\perp)$ the interpolation expression

$$J_{ac}(\vec{q}_\perp = (0, q_\zeta)) = \frac{8(v_{2,c}^A)^2 \sin^2(q_\zeta \frac{c}{2})}{q_\zeta^2 c_{44} abc}, \quad (5.4)$$

which coincides with Eq. (4.29) at \vec{q}_Γ and vanishes at \vec{q}_Z . While for KC₆₀, with small polarizability of the K⁺ ion, the direct interchain interaction $J_{QQ}(\vec{q}_Z)$ dominates and hence leads to $Pmnn$, for RbC₆₀ and even more for CsC₆₀, the alkali mediated interaction $J_{ep}(\vec{q}_\Gamma)$ is most important and leads to the structure $I2/m$. This structure is monoclinic and indeed one has measured small deviations of the (\vec{b}, \vec{c}) angle from 90° [13,14]. The present theory accounts for such shears. We rewrite expression (4.26) for $\vec{q}_\perp = (0, q_\zeta)$ as

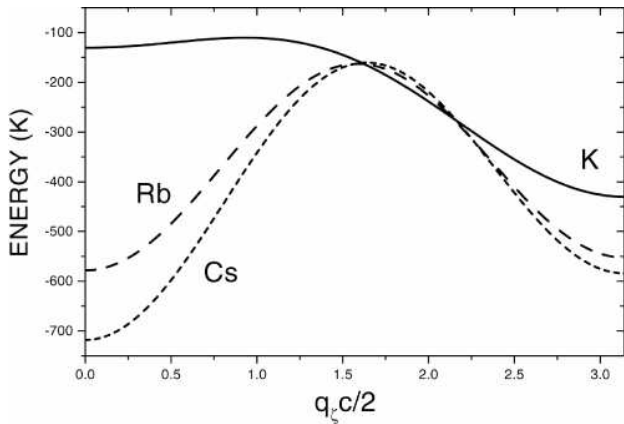


FIG. 3. Interchain energy $J(\vec{q}_\perp)$, units K.

$$q_\zeta s_\eta^\dagger(0, 0, q_\zeta) = \frac{2i\sqrt{m}v_{2,c}^A}{abc_{44}} \sqrt{N_1} S_2^\dagger(0, q_\zeta). \quad (5.5)$$

We observe that

$$\lim_{q_\zeta \rightarrow 0} i q_\zeta s_\eta(0, 0, q_\zeta) = \sqrt{mN} \epsilon_{\zeta\eta}, \quad (5.6)$$

where $\epsilon_{\zeta\eta}$ are the homogeneous shears, and $N = N_1 N_c$ is the number of unit cells. Taking then the limit $q_\zeta \rightarrow 0$ in Eq. (5.5), we get by using Eq. (4.43)

$$\epsilon_{\zeta\eta} = \frac{2v_{2,c}^A}{abc_{44}} \sigma \quad (5.7)$$

where σ is the order parameter amplitude. We see that ferrorotational order induces ζ , η shears, in accordance with the monoclinic space group $I2/m$. With the numerical values of $v_{2,c}^A$ from Table IV, the lattice parameters of Table I and assuming $\sigma = 1$, we obtain for $\epsilon_{\zeta\eta}$ the values of 0.476° and 0.483° for RbC_{60} and CsC_{60} respectively. The deviations from 90° of the (\vec{b}_o, \vec{c}_o) angle measured experimentally are 0.316° [14] and 0.180° [13] for Rb and CsC_{60} respectively.

VI. CONCLUSIONS

In comparing the numerical values of the various contributions of the total interaction energies in Tables V and VI we come to the conclusion that the quadrupolar electronic polarizability mediated interaction $J_{ep}(\vec{q}_\perp)$ and the direct quadrupolar interaction $J_{QQ}(\vec{q}_\perp) = J_{QQ}^C(\vec{q}_\perp) + J_{QQ}^W(\vec{q}_\perp)$ are the determining factors for the structures $Pmnn$ or $I2/m$, while the TR mediated interaction $J_{ac}(\vec{q}_\perp)$ plays quantitatively a negligible role. The direct quadrupolar interaction, both of van der Waals and Coulomb type, is always attractive and maximum at $\vec{q}_\perp = \vec{q}_Z$ and hence favors the antiferrorotational structure, in agreement with the space group $Pmnn$ for pressure polymerized C_{60} [23,24] and

for polymerized KC_{60} [7,12]. Notice that the values of $J_{QQ}(\vec{q}_Z)$ for all three AC_{60} compounds are rather close together, and hence there is no way to explain the different structure $I2/m$ for RbC_{60} [12,14] and CsC_{60} [13] by the direct interchain coupling via C_{60} monomers, the only difference between the three compounds being the lattice constants. The role of the alkalis has to be more specific [20] than just providing different lattice spacings.

Since the values of $J_{ac}(\vec{q}_\Gamma)$ are rather small and similar for the three compounds (Table V), the only decisive interaction allowing to discriminate between KC_{60} and RbC_{60} , CsC_{60} , is the quadrupolar polarizability of the cations, introduced in Sect. IV. Here we do not invoke the quadrupolar polarizability of the inner shells with small ionic radii but the quadrupole formation due to excited d -states [20] which carry a residual electronic charge. The average radii d_A of these states, calculated in Appendix C and quoted in Table IV, are considerably larger than the ionic radii of K^+ , Rb^+ , Cs^+ in conventional compounds like the alkali halides or like the ionic crystals with small molecular ions (alkali-cyanides, -nitrites). Within our view the large interstitial space available for the “octahedral” alkalis in AC_{60} compounds is a prerequisite for the existence and partial occupancy of these d -states in the solid. In that respect the alkali-fullerides are unique ionic solids, and we expect that the excited d -states are relevant for an understanding of the electromagnetic properties [3]. Notice that in the present approach RbC_{60} and CsC_{60} are similar because their average radii of excited $4d$ - and $5d$ -states respectively are close, while KC_{60} with an excited $3d$ -state has a considerably smaller value of d_A . A same trend is also present in the atomic radii of the transition metals Sc, Y and the inner transition metal La, with $3d^1$, $4d^1$ and $5d^1$ electrons respectively, with atomic radii 1.64 \AA , 1.82 \AA and 1.88 \AA respectively.

Within the present work we have assumed a model of rigid polymer chains which describes the structures $Pmnn$ and $I2/m$. The assumption of rigid chains has to be abandoned if one wants to take into account a modulation of electronic and structural properties along the orthorhombic \vec{a} axis. In fact the interaction of electric quadrupoles between C_{60} monomers along a same chain immediately suggests an antiferro-orientational structure along the chains. However such an extension is not yet sufficient to understand the recently discovered superstructure $(\vec{a} + \vec{c}, \vec{b}, \vec{a} - \vec{c})$ below $T = 50 \text{ K}$ in KC_{60} [15]. Here again the alkalis seem to play a specific role.

ACKNOWLEDGMENTS

We acknowledge useful discussions with K. Knorr, P. Launois and R. Moret. This work has been financially supported by the Fonds voor Wetenschappelijk Onderzoek, Vlaanderen, and by the Bijzonder Onderzoeksfonds, Universiteit Antwerpen, UIA.

APPENDIX A:

In the cubic phase the elastic part of the free energy per formula unit AC₆₀ reads [25]

$$U_{el} = \frac{V_c}{2} [c_{11} (\epsilon_{xx}^2 + \epsilon_{yy}^2 + \epsilon_{zz}^2) + 2c_{12} (\epsilon_{xx}\epsilon_{yy} + \epsilon_{yy}\epsilon_{zz} + \epsilon_{zz}\epsilon_{xx}) + 4c_{44} (\epsilon_{xy}^2 + \epsilon_{yz}^2 + \epsilon_{zx}^2)]. \quad (\text{A1})$$

Here $V_c = a_c^3/4$ is the volume of the primitive unit cell, a_c is the cubic lattice constant, c_{ij} are the elastic constants (we use the Voigt notation) and ϵ_{ij} are the lattice deformations. Performing a rotation of the cubic system of axes (x, y, z) to an orthorhombic system (ξ, η, ζ) , where ξ corresponds to the cubic [110] direction, η to $[\bar{1}10]$ and ζ to [001], we get

$$U_{el} = \frac{V_c}{2} [c_{11}^o (\epsilon_{\xi\xi}^2 + \epsilon_{\eta\eta}^2) + c_{33}^o \epsilon_{\zeta\zeta}^2 + 2c_{12}^o \epsilon_{\xi\xi}\epsilon_{\eta\eta} + 2c_{13}^o \times (\epsilon_{\xi\xi}\epsilon_{\zeta\zeta} + \epsilon_{\eta\eta}\epsilon_{\zeta\zeta}) + 4c_{66}^o \epsilon_{\xi\eta}^2 + 4c_{55}^o (\epsilon_{\xi\zeta}^2 + \epsilon_{\eta\zeta}^2)]. \quad (\text{A2})$$

Here the orthorhombic elastic constants c_{ij}^o are related to the cubic elastic constants by $c_{11}^o = (c_{11} + c_{12} + 2c_{44})/2$, $c_{12}^o = (c_{11} + c_{12} - 2c_{44})/2$, $c_{33}^o = c_{11}$, $c_{23}^o = c_{12}$, $c_{13}^o = c_{12}$, $c_{66}^o = (c_{11} - c_{12})/2$, $c_{55}^o = c_{44}$. Polymerization acts as a compression along [110], i. e. along ξ . The corresponding surface forces are described by the boundary condition [25]

$$F_i = \sigma_{ik} n_k, \quad (\text{A3})$$

where σ_{ik} is the elastic stress tensor (indices i, k run over the orthorhombic axes ξ, η, ζ); \vec{n} is the normal to the surface. Using

$$\sigma_{ik} = \frac{1}{V_c} \frac{\partial U_{el}}{\partial \epsilon_{ik}}, \quad (\text{A4})$$

and observing that $\vec{F} = (-K, 0, 0)$, where $K > 0$ is the strength of the compressional force, we obtain

$$\sigma_{\xi\xi} = c_{11}^o \epsilon_{\xi\xi} + c_{12}^o \epsilon_{\eta\eta} + c_{13}^o \epsilon_{\zeta\zeta} = -K. \quad (\text{A5a})$$

Since there are no lateral forces, $\sigma_{\eta\eta} = 0$ and $\sigma_{\zeta\zeta} = 0$, which leads to

$$c_{11}^o \epsilon_{\eta\eta} + c_{12}^o \epsilon_{\xi\xi} + c_{13}^o \epsilon_{\zeta\zeta} = 0, \quad (\text{A5b})$$

$$c_{33}^o \epsilon_{\zeta\zeta} + c_{13}^o \epsilon_{\xi\xi} + c_{23}^o \epsilon_{\eta\eta} = 0, \quad (\text{A5c})$$

and $\sigma_{\xi\eta} = 0$, $\sigma_{\zeta\eta} = 0$, $\sigma_{\xi\zeta} = 0$ lead to $\epsilon_{\xi\eta} = 0$, $\epsilon_{\zeta\eta} = 0$, $\epsilon_{\xi\zeta} = 0$. Solving the system of equations (A5a)-(A5c) we get the deformations that are quoted in Eqs. (2.1a)-(2.1c).

APPENDIX B:

TABLE VII. Born-Mayer-van der Waals potential constants for the interactions between the various types of ICs (a stands for ‘‘atom’’, db for ‘‘double bond IC’’ and sb for ‘‘single bond IC’’). The factors $\frac{1}{9}$ and $\frac{1}{3}$ arise from the threefold multiplicity of the double bond ICs. For comparison with earlier work [34,50], C_1 is expressed in units 3.745×10^7 K and B in units 3.054×10^5 K \AA^6 , C_2 is given in \AA^{-1} .

	$a - a$	$db - db$	$sb - sb$	$a - db$	$a - sb$	$db - sb$
C_1	0.864	$\frac{1}{9} \times 0.259$	0.158	$\frac{1}{3} \times 0.169$	0.169	0
C_2	3.6	3.2	3.6	3.4	3.6	0
B	2.1	0	0	0	0	0

1. Born-Mayer and van der Waals Interactions between C₆₀ Monomers

A C₆₀ monomer in AC₆₀ (A=K, Rb, Cs) is described by a rigid cluster of interaction centers (ICs). The ICs refer to pair potentials between monomers on separate chains. In addition to the 60 carbon atoms, three ICs per double bond (at positions $L/2$ and $\pm L/4$, where L is the bond length) and one IC per single bond (located at the bond center) are considered. Following [34] we consider van der Waals potentials of type (3.5), where the potential parameters C_1 , C_2 and B depend on the type of ICs. Numerical values are given in Table VII. The comparison of experimental X-ray diffuse scattering results with theoretical predictions based on various intermolecular potentials, shows that such a model has its merits [42]. However the transition temperature T_c for the phase change $Fm\bar{3}m \rightarrow Pa\bar{3}$ obtained by potentials used in [34] is much too large [42,43] in comparison with the experimental value $T_c \approx 250$ K. It is then necessary to adjust the potential parameters. A potential is considered satisfactory if it reproduces the transition temperature and the experimental crystal field [44] in the orientationally disordered phase of C₆₀. The potential parameters of Table VII give $T_c = 252$ K and crystal field expansion parameters $w_6 = 346.3$, $w_{10} = -84.1$, $w_{12,1} = -82.9$, $w_{12,2} = -378.6$ for the disordered phase of solid C₆₀.

2. Born-Mayer and van der Waals Interactions between a C₆₀ Monomer and an Alkali Atom

Here we let the alkali atom interact with the 60 carbon atoms of the C₆₀ monomer. We take again the pair potential of the form of Eq. (3.5). Numerical values for the potential constants are quoted in Table VIII. These values are derived from the homoatomic interaction potential constants: for C–C the $a - a$ values of Table VII were used, for K–K and Rb–Rb the values of Ref. [45] were taken, and for Cs–Cs an extrapolation of the K–K and Rb–Rb values based on the ratios of the ionic radii of K^+ , Rb^+ and Cs^+ was made.

TABLE VIII. Born-Mayer-van der Waals potential constants for the interaction between a carbon atom and an alkali atom.

	units	C-K	C-Rb	C-Cs
C_1	10^7 K	2.43	3.59	4.96
C_2	\AA^{-1}	3.28	3.29	3.32
B	10^5 K \AA^6	3.36	5.26	8.23

APPENDIX C:

To calculate the portion of the charge located inside the interstitial sphere precisely, one should perform an electron band structure calculation of AC₆₀. However, some conclusions can be made on the basis of a general consideration. In the tight-binding approximation we expect that the electron wave function of a band electron at an alkali site \vec{n} , $\psi_A(\vec{k}, \alpha)|_{\vec{n}}$, is expanded in terms of local s and d functions, i.e.

$$\psi_A(\vec{k}, \alpha)|_{\vec{n}} = \frac{1}{\sqrt{N}} e^{i\vec{k}\cdot\vec{X}(\vec{n})} \left[\gamma_{00}(\vec{k}, \alpha) R_s(r) Y_0^0 + \sum_{m=-2}^2 \gamma_{2m}(\vec{k}, \alpha) R_d(r) Y_2^m(\hat{r}) \right], \quad (\text{C1})$$

where $R_s(r)$ and $R_d(r)$ are the radial parts of s and d states of the alkali, respectively. (N is the total number of sites in the crystal.) Here we are speaking about $4s$ and $3d$ electron states for K, $5s$ and $4d$ states for Rb, and $6s$ and $5d$ states of Cs. The s and d coefficients $\gamma_{lm}(\vec{k}, \alpha)$ (i.e. $\gamma_{00}(\vec{k}, \alpha)$ and $\gamma_{2m}(\vec{k}, \alpha)$) are found by solving a secular equation for the band electron with the wave vector \vec{k} and the band number α . The inclusion of the d -states in $\psi_A(\vec{k}, \alpha)|_{\vec{n}}$ is logical since for a neutral K, Rb and Cs atom the d -shell corresponds to the first excited electron level. The resulting charge distribution inside the sphere at the site \vec{n} can be computed by summing up the density of all extended states \vec{k}, α below the Fermi energy, $E(\vec{k}, \alpha) \leq E_F$. The charge at the alkali site is small but not zero and we believe that $|\gamma_{00}^0(\vec{k}, \alpha)|^2 \sim 0.1$, $|\gamma_{2m}^m(\vec{k}, \alpha)|^2 \sim 0.1$. It is important that the wave function $\psi_A(\vec{k}, \alpha)$ has nonzero matrix elements of quadrupolar charge density. To demonstrate this, we consider quadrupole components of the electronic density associated with SARFs $S_\Lambda(\hat{r})$, where Λ refers either to the two components ($k = 1, 2$) of E_g symmetry or to the three components ($k = 1, 2, 3$) of T_{2g} symmetry, i.e. $\Lambda = (l = 2, \Gamma, k)$, where $\Gamma = E_g$ or T_{2g} . In Ref. [46] it has been shown that the operator of quadrupolar density of conduction electrons reads

$$\rho_\Lambda^{l_1 l_2}(\vec{q}) = \frac{1}{\sqrt{N}} \sum_{\alpha, \beta} \sum_{\vec{k}} a_{\vec{k}\alpha}^\dagger a_{\vec{k}-\vec{q}\beta} c_{\Lambda l_1 l_2}(\vec{k}, \alpha; \vec{k} - \vec{q}, \beta), \quad (\text{C2})$$

where $l_1, l_2 = 0$ or 2 (s and d states), and $a_{\vec{k}\alpha}^\dagger, a_{\vec{k}\alpha}$ are creation and annihilation operators for one electron in

the state (\vec{k}, α) . Here

$$c_{\Lambda l_1 l_2}(\vec{k}, \alpha; \vec{p}, \beta) = \sum_{m_1, m_2} \gamma_{l_1 m_1}^*(\vec{k}, \alpha) \gamma_{l_2 m_2}(\vec{p}, \beta) \times c_\Lambda(l_1 m_1, l_2 m_2). \quad (\text{C3})$$

with the quadrupolar matrix elements

$$c_\Lambda(l_1 m_1, l_2 m_2) = \int Y_{l_1}^{m_1 *}(\Omega) S_\Lambda(\Omega) Y_{l_2}^{m_2}(\Omega) d\Omega. \quad (\text{C4})$$

Some coefficients $c_\Lambda(l_1 m_1, l_2 m_2)$ are different from zero for certain $d-d$ and $d-s$ transitions as has been shown in Ref. [46] within a more general context (see there Eq. (3.21) for $s-d$ transitions, and Table I for $d-d$ transitions with $\Lambda = (T_{2g}, k)$). From the latter observation we conclude that if there is an appreciable weight of d -states in $\psi_A(\vec{k}, \alpha)|_{\vec{n}}$, Eq. (C1), then the alkalis acquire a quadrupole moment. (In order to obtain the operator of the quadrupolar moment for the ground state of AC₆₀ we put $\vec{q} = \vec{k} - \vec{p} = \vec{0}$ and $\alpha = \beta$ in Eqs. (C2) and (C3).) This consideration gives a microscopic support for the concept of quadrupolar polarizability of alkalis introduced in Ref. [20]. It is clear that the quadrupolar moment of alkalis depends on the coefficients $\gamma_{00}(\vec{k}, \alpha)$, $\gamma_{2m}(\vec{k}, \alpha)$. In principle, the secular equation for the coefficients should also take into account the bilinear quadrupole-quadrupole interaction with the polymer chains of C₆₀ molecules. In practice, however, such calculation would be very difficult to implement. Instead, following Ref. [20] one can introduce phenomenologically quadrupolar moments of alkalis and then optimize their interactions with the neighboring polymer chains. In this work we use a simple model with two point charges q_A at distances $\pm d_A$ from the alkali center. Here d_A is an average d -shell radius which is found as

$$d_A = \langle r \rangle_d = \int_0^\infty \mathcal{R}_d(r') r'^3 dr'. \quad (\text{C5})$$

The radial functions \mathcal{R}_d and the average radii (d_K, d_{Rb}, d_{Cs}) were calculated numerically. We have employed a relativistic atomic program for self-consistent-field calculations of K^+ , Rb^+ and Cs^+ with the local density approximation (LDA) of exchange according to Barth-Hedin [47]. Since the ionicity of alkalis is close to +1, $\mathcal{R}_d(r)$ corresponds to the virtual (almost empty) $3d_{3/2}$ shell for K, to the virtual $4d_{3/2}$ level for Rb and to the virtual $5d_{3/2}$ level for Cs. The role of excited d -functions has been discussed by Murrel [48] and by Niebel and Venables [49] in connection with the problem of explaining the observed crystal structure of the rare gas solids.

On the other hand, as it has been shown in Ref. [46] there is electronic on-site interaction which is proportional to the square of the quadrupolar moment (see Eq. (3.14a) of Ref. [46]). This interaction gives rise to the intraionic self-energy g_A introduced in Eq. (6) of Ref. [20]

and Eq. (4.38) of the present work. Upon uniform expansion or contraction of the electron density around an alkali, the strength of it scales as $1/d_A$.

-
- [1] M.S. Dresselhaus, J. Dresselhaus, and P.C. Eklund, *Science of Fullerenes and Carbon Nanotubes* (Academic Press, New York, 1995).
- [2] H. Kuzmany, B. Burger, and J. Kürti, in *Optical and Electronic Properties of Fullerenes and Fullerene-Based Materials*, edited by J. Shinar, Z.V. Vardeny, and Z.H. Kafafi (Marcel Dekker, New York, 2000).
- [3] L. Forró and L. Mihály, Rep. Progr. Phys. **64**, 649 (2001).
- [4] J. Winter and H. Kuzmany, Solid State Commun. **84**, 935 (1992); Q. Zhu, O. Zhou, J.E. Fischer, A.R. McGhie, W.J. Romanov, R.M. Strongin, M.A. Cichy, and A.B. Smith III, Phys. Rev. B **47**, 13948 (1993).
- [5] S. Pekker, L. Forró, L. Mihály, and A. Jánossy, Solid State Commun. **90**, 349 (1994).
- [6] O. Chauvet, G. Oszlányi, L. Forró, P.W. Stephens, M. Tegze, G. Faigel, and A. Jánossy, Phys. Rev. Lett. **72**, 2721 (1994).
- [7] P.W. Stephens, G. Bortel, G. Faigel, M. Tegze, A. Jánossy, S. Pekker, G. Oszlányi, and L. Forró, Nature **370**, 636 (1994).
- [8] B. Renker, H. Schober, F. Gompf, R. Heid, and E. Ressouche, Phys. Rev. B **53**, 14701 (1996); B. Renker, H. Schober, and R. Heid, Appl. Phys. A **64**, 271 (1997).
- [9] A.M. Rao, P. Zhou, K.-A. Wang, G.T. Hager, J.M. Holden, Y. Wang, W.-T. Lee, X.-X. Bi, P.C. Eklund, and D.S. Cornett, Science **259**, 955 (1993).
- [10] F. Bommeli, L. Degiorgi, P. Wachter, O. Legeza, A. Chauvet, G. Jánossy, O. Oszlányi, and L. Forró, Phys. Rev. B **51**, 14794 (1995).
- [11] H. Alloul, V. Brouet, E. Lafontaine, L. Malier, and L. Forró, Phys. Rev. Lett. **76**, 2922 (1996).
- [12] P. Launois, R. Moret, J. Hone, and A. Zettl, Phys. Rev. Lett. **81**, 4420 (1998).
- [13] S. Rouzière, S. Margadonna, K. Prassides, and A.N. Fitch, Europhys. Lett. **51**, 314 (2000).
- [14] A. Huq, P.W. Stephens, G.M. Bendele, and R.M. Ibberson, Chem. Phys. Lett. **347**, 13 (2001).
- [15] C. Coulon, A. Pénicaud, R. Clérac, R. Moret, P. Launois, and J. Hone, Phys. Rev. Lett. **86**, 4346 (2001).
- [16] S.C. Erwin, G.V. Krishna, and E.J. Mele, Phys. Rev. B **51**, 7345 (1995).
- [17] K. Tanaka, T. Saito, Y. Oshima, T. Yamabe, H. Kobayashi, Chem. Phys. Lett. **272**, 189 (1997).
- [18] V.L. Aksenov, V.S. Shakmatov, and Y.A. Osipyan, JETP Lett. **62**, 428 (1995); eidem JETP Lett. **64**, 120 (1996).
- [19] A.V. Nikolaev, K. Prassides, and K.H. Michel, J. Chem. Phys. **108**, 4912 (1998).
- [20] K.H. Michel and A.V. Nikolaev, Phys. Rev. Lett. **85**, 3197 (2000).
- [21] A.V. Nikolaev and K.H. Michel, Solid State Commun. **117**, 739 (2001).
- [22] P. Launois, R. Moret, E. Llusca, J. Hone, and A. Zettl, Synth. Metals **103**, 2357 (1999).
- [23] V.A. Davidov, L.S. Kashevarova, A.V. Rakhmanina, A.V. Dzyabchenko, V.N. Agafonov, P. Dubois, R. Ceolin, and H. Szwarc, JETP Lett. **66**, 120 (1997).
- [24] R. Moret, P. Launois, P.-A. Persson, and B. Sundqvist, Europhys. Lett. **40**, 55 (1997).
- [25] L.D. Landau and E.M. Lifshitz, *Theory of Elasticity* (Pergamon, New York, 1986).
- [26] H. Schober, A. Tölle, B. Renker, R. Heid, and F. Gompf, Phys. Rev. B **56**, 5937 (1997).
- [27] H.M. Guerrero, R.L. Cappelletti, D.A. Neumann, and T. Yildirim, Chem. Phys. Lett. **297**, 265 (1998).
- [28] H.M. James and T.A. Keenan, J. Chem. Phys. **31**, 12 (1959).
- [29] W. Press and A. Hüller, Acta Crystallograph. A **29**, 252 (1973).
- [30] M. Yvinec and R.M. Pick, J. Phys. (France) **41**, 1045 (1980).
- [31] W. Press, Acta Crystallogr. A **29**, 257 (1973).
- [32] M. Sprik, A. Cheng, and M.L. Klein, J. Phys. Chem. **96**, 2027 (1992).
- [33] R. Heid, Phys. Rev. B **47**, 15912 (1993).
- [34] D. Lamoen and K.H. Michel, J. Chem. Phys. **101**, 1435 (1994).
- [35] R.C. Haddon, L.E. Brus, and K. Raghavachari, Chem. Phys. Lett. **125**, 459 (1986).
- [36] T.M. de Swiet, Y.L. Yarger, T. Wagberg, J. Hone, B.J. Gross, M. Tomaselli, J.J. Titman, A. Zettl, and M. Mehring, Phys. Rev. Lett. **84**, 717 (2000).
- [37] R.M. Lynden-Bell and K.H. Michel, Revs. Mod. Phys. **66**, 721 (1994).
- [38] J. Yu, L. Bi, R.K. Kalia, and P. Vashishta, Phys. Rev. B **49**, 5008 (1994).
- [39] A. Hüller, Z. Physik **254**, 456 (1972); A. Hüller and J.W. Kane, J. Chem. Phys. **61**, 3599 (1974).
- [40] W. Krätschmer, L.D. Lamb, K. Fostiropoulos, and D.R. Huffman, Nature **347**, 354 (1990).
- [41] R.A. Cowley, W. Cochran, B.N. Brockhouse, and A.D.B. Woods, Phys. Rev. **131**, 1030 (1963); R. Migoni, H. Bilz, and D. Bäuerle, Phys. Rev. Lett. **37**, 1155 (1976).
- [42] P. Launois, S. Ravy, and R. Moret, Phys. Rev. B **55**, 2651 (1997).
- [43] K.H. Michel and J.R.D. Copley, Z. Phys. B **103**, 369 (1997).
- [44] P.C. Chow, X. Jiang, G. Reiter, P. Wochner, S.C. Moss, J.D. Axe, J.C. Hanson, R.K. McMullen, R.L. Meng, and C.W. Chu, Phys. Rev. Lett. **69**, 2943 (1992); W.I.F. David, R.M. Ibberson, and T. Matsuo, Proc. R. Soc. London Ser. A **442**, 129 (1993); P. Schiebel, K. Wulf, W. Prandl, G. Heger, R. Papoular, and W. Paulus, Acta Crystallogr. A **52**, 176 (1996).
- [45] M. Ferrario, I.R. McDonald, and M.L. Klein, J. Chem. Phys. **84**, 3975 (1986).
- [46] A.V. Nikolaev and K.H. Michel, Eur. Phys. J. B, **17**, 15 (2000).
- [47] V. von Barth and L. Hedin, J. Phys. C **5**, 1629 (1972).
- [48] J.N. Murrell, Discuss Faraday Soc., **40**, 130 (1965).
- [49] K.F. Niebel and J.A. Venables, in *Rare Gas Solids*, M.L. Klein and J.A. Venables eds., Academic Press, London,

1976, p. 558.

- [50] B.J. Nelissen, P.H.M. van Loosdrecht, M.A. Verheijen, A. van der Avoird, and G. Meijer, *Chem. Phys. Lett.* **207**, 343 (1993).